Renewable and Sustainable Energy Reviews 19 (2013) 613–628

Contents lists available at SciVerse ScienceDirect

Renewable and Sustainable Energy Reviews

journal homepage: www.elsevier.com/locate/rser

Review of primary control strategies for islanded microgrids with power-electronic interfaces

T.L. Vandoorn *, J.D.M. De Kooning, B. Meersman, L. Vandevelde

Department of Electrical Energy, Systems and Automation (EESA), Ghent University, Sint-Pietersnieuwstraat 41, B-9000 Ghent, Belgium

A R T I C L E I N F O

Article history:
Received 7 September 2012
Accepted 20 November 2012
Available online 20 December 2012

Keywords:
Microgrids
Islanded operation
Power-electronic converters
Primary control

A B S T R A C T

To cope with the increasing share of distributed generation (DG) units in the distribution network, a coordinated integration is required. An aggregation of DG units, loads and storage elements into microgrids with proper control strategies can provide this coordination. As most DG units are power-electronically interfaced to the grid, specific control strategies have been developed for the converter interfaces of the DG units in islanded microgrids. This paper provides a survey of these control strategies and shows detailed figures of the control schemes.

Contents

* Corresponding author. Tel.: +32 9 264 34 22; fax: +32 9 264 35 82.
E-mail address: Tine.Vandoorn@UGent.be (T.L. Vandoorn).

1364-0321/$ - see front matter © 2012 Elsevier Ltd. All rights reserved.
http://dx.doi.org/10.1016/j.rser.2012.11.062

1. Introduction

Modern power networks are subject to several challenges: load growth, changes in geographical distribution of the generators, an aging energy infrastructure, new environmental policies and economic pressures. The historical solution to deal with these issues, i.e., upgrading the infrastructure, can solve the first three issues, but is constrained by the latter two [1]. Also, extension of the transmission network is usually not possible, or has long lead times, due to the "not-in-my backyard" attitude of the local community. Distributed generation (DG) can ease the pressure on transmission system capacity by supplying some of the load. However, DG connection in the conventional "fit-and-forget" strategy increasingly conflicts with the primary objective of the power system, i.e., to deliver reliable energy supply. The intermittent nature of an increasing share of generators and the increased share of not-actively dispatched units can jeopardize the stability of the system. Also, most DG units are connected to weaker distribution networks, in which voltage and congestion problems increasingly occur. Therefore, the microgrid concept has been presented as a potential means to combat problems by the unconventional behavior of DG and to increase the DG penetration [1].

By presenting a systematic organization and a coordinated integration of DG in the network, the microgrid has more capacity and control flexibility to fulfil system reliability and power quality requirements compared to a single DG unit [2]. Depending on the location and capacity of the DG units, the microgrids operate at medium or low-voltage distribution level, where this paper focusses on low-voltage microgrids. As it presents itself to the utility as a dispatchable load, the microgrid behaves as a controllable entity. This offers important scaling benefits for the distribution network operator. It also enables the (small) microgrid elements to participate in the electricity markets. Aggregating different kinds of DG units, storage elements and loads in a microgrid can, for example, reduce the prediction errors of the generated wind power by changing the load profile or the output of other generators.

Microgrids can operate in grid-connected mode or islanded mode. In islanded microgrids, the units are responsible for the voltage control as well as the power sharing and balancing. The role of the power-sharing feature is to ensure that all modules share the load according to their ratings and availability of power from their energy source. As most DG units are interfaced to the grid through power-electronic converters, islanded microgrids require specific converter control strategies, an overview of which is given in this paper. Initially, paralleled control in the islanded operation originates from uninterruptible power supply (UPS) systems. In [3], it is applied in isolated microgrids. Both communication-based control strategies and controllers without communication can be used.

The units can be classified in grid-forming (voltage-controlled) and grid-following (current-controlled) DG units. In an islanded microgrid, at least one grid-forming DG unit is required as otherwise, there is no voltage reference and no control to maintain the power balance. In the single master operation, one unit operates as a grid-forming inverter. The other units operate as grid-following units [3]. In the multi-master operation, more than one unit is grid-forming, possibly combined with grid-following inverters [3]. The grid-forming units are responsible for reacting on the fast load variations dependent on their ratings, while grid-following units inject a pre-determined amount of power into the network.

2. Classification

As discussed earlier, the DG units can be classified in grid-forming or grid-following units. The mainly used control strategies for grid-following inverters are discussed in [4]. This paper focusses on the control strategies for grid-forming converters which take part in the power sharing and balancing of the microgrid. Of course, next to these grid-forming converters, grid-following converters can be present as well, which can be regarded as negative loads.

A further classification of the grid-forming control strategies can be based on the communication requirements. Communication-based controllers include master/slave control and central control. Controllers without communication are generally based on the droop concept. Of course, these control schemes can be overlayed by a secondary, slower control, that changes the set-points of the units using communication. This paper does not include secondary and tertiary controllers. An overview of the primary controllers, that are responsible for the microgrid stability, is given, including detailed control schemes.

3. Simplest method to connect inverters in parallel

The simplest method to connect inverters in parallel is to physically add an inductor at the output of the inverters [5]. However, a bulky inductor increases the size and cost of the system. In case the load current contains harmonics, the output voltage will also be strongly distorted by the inductors. Another implementation is to include a series resistor at the output of the individual sources [6]. The main disadvantage is the increase of power losses.

With these output impedances and in case of equal terminal impedances and output voltages, the output current of the converters will be shared equally. However, in real situations, the parameters of the converters have deviations. The load sharing is sensitive to phase angle differences, line impedances, output LC filter values and so on. When two power sources are only connected through a line inductance, the smallest phase or amplitude deviation causes circulating currents between the converters and, hence, a power sharing that is not controlled. This sensitivity is the reason why converters controlled at fixed frequency f and voltage V cannot operate in parallel [7]. There is always a voltage difference caused by the tolerance of the sensors, references, temperature drift, aging and crystal differences.

4. Control strategies with communication

The control strategies with communication achieve good voltage regulation and power sharing. Also, opposed to the droop controllers discussed further, the output voltage is generally closer to its nominal value. However, these strategies need communication lines between the modules. Communication lines are expensive and vulnerable, especially for long distances. They could also reduce the system reliability and expandability and limit the flexibility of the system.

4.1. Central control/concentrated control

In the central control method, a central controller coordinates the power-electronic interfaces in the microgrid to maintain the balance in active power P and reactive power Q in steady-state conditions [1]. A communication link between the central controller and each unit is required. Central control has the advantage of using simple control algorithms in the converters. However, large expenses for the communication lines and a supervisory control center are required. Hence, central control is difficult to implement in highly distributed and large systems [1]. Central control also makes it difficult to expand the system [8].

A possibility for central control is to use the single master operation, with one unit in the grid-forming mode. The power sharing can be achieved by using a central controller that

measures the total load power and distributes the weighted value (for example, with weighting according to the ratings of the DG units) to all units. The other DG units operate in grid-following mode, following the grid voltage and changing the output power according to the centrally communicated signals. The synchronization can be achieved by using a phase locked loop (PLL). However, it is difficult to achieve a fast response for power distribution control due to the inherently relatively slow response of the PLL [9].

The *central-limit control* (*CLC*) is discussed in [10–12] and the control scheme is depicted in Fig. 1. The power sharing and voltage regulation are controlled centrally and the subsequent commands are distributed through a communication link. A central controller defines the set-value of the current for each module. This reference current i_{ref} is a fraction of the load current i_{load} that is measured by the central controller. For N equal modules $i_{ref} = i_{load}/N$, i.e., the central-limit reference current (the mean value of all source currents). It is also possible to connect units with different power-ratings to the system. Then, for each unit, a different reference current is needed and the central controller uses individual weighting functions instead of $1/N$. Of course, the sum of the N weighting functions should be equal to one. The central controller also determines a voltage correction term v_e to control the measured load voltage v_o to its reference value v_{ref} and communicates this voltage v_e to all modules. To determine the central v_{ref}, several options exist as is discussed in [11]. The local controllers of each module control their output current to the reference current received from the central controller. The output v_c of the current controller is added to v_e. The output voltage of each module is generated from $v_e + v_c$ and generated by using pulse-width modulation (PWM). The shared signals that require a communication link are v_e and i_{ref}.

An advantage of this method is that current sharing is forced during all times, also during transients. During transients, the current loop is responsible for maintaining power sharing between the modules. The voltage loop will recover the voltage. With this method, accurate power sharing is achieved in steady-state as well as during transients, opposed to the master/slave control schemes in which the master unit delivers most of the compensation current during the transients. The main disadvantage is that both v_e and i_{ref} have to be distributed to all converters by using a high-bandwidth communication link to synchronize the units [13].

Note that the line impedances are generally not considered explicitly in this paragraph (Section 4), opposed to in Section 5 consisting of controllers without communication. Neglecting the line impedances in the control strategies is a significant disadvantage, as the definition of load voltage v_o becomes unclear when the microgrid consists of a feeder with multiple DG units and loads.

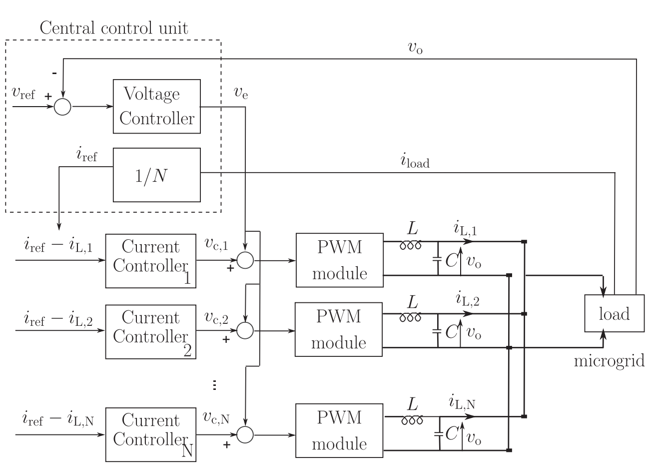

Fig. 1. Central-limit control principle.

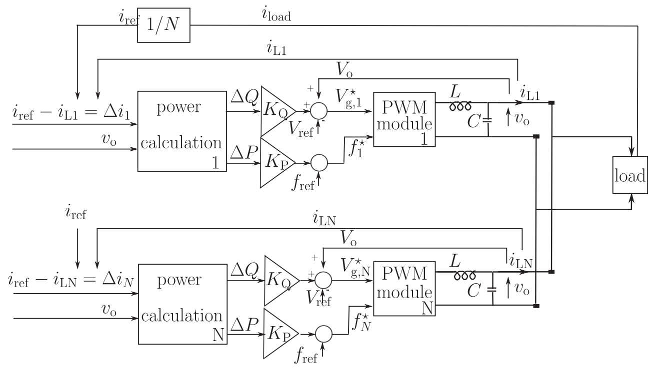

Fig. 2. Power deviation control.

The *power deviation method* is based on the theory that the active and reactive power are separately determined by the phase angle and amplitude of each module's output voltage, respectively. In this control method, the load current i_{load} is (centrally) measured and divided by the number of operating inverters N (or by using a weighting factor) to obtain i_{ref}. This information is fed to all modules. From $i_{ref} - i_{L,i}$ and v_o, the power deviation, i.e., the active component ΔP and the reactive component ΔQ, are evaluated. In [14] and Fig. 2 the inverters are connected to the common bus via a series inductance. As will be discussed further, in inductive networks, the active power P is predominantly defined by the power angle θ, and the reactive power Q is mainly determined by the inverter voltage amplitude v_o. The power angle is dynamically controlled by slightly changing the inverter frequency. The reactive power deviation ΔQ, the common grid voltage reference v_{ref} and inverter output voltage v_o determine the set value $v_g^{\star}$ of the inverters. The active power deviation ΔP and the frequency reference, determine the new frequency set-value .

4.2. Master/slave control

In this control strategy, both voltage and current controllers are used. In central-limit control, the converters share the total load current by using weighting factors. A disadvantage is, thus, that if the sum of these factors differs from one, due to for example the shut down of a unit or a programming fault, the load current is not supplied properly [12]. In master/slave control on the other hand, the master only has voltage control, no current control. Hence, this unit delivers the transient current and compensates for wrong weighting factors. The master module is responsible for output voltage regulation and to specify the reference current of each inverter. The slave units track the current command provided by the master to achieve an equal current distribution. It is well-known that a master–slave control can realize excellent current sharing performance with easy implementation, even with non-identical modules. However, master/slave control does not achieve redundancy as the slave units depend on the master module. Another drawback is that as the master output current is not controlled, high output current overshoot during transients can occur. The slave units react slower to the transient current demand such that the master needs to provide the compensation current [13]. Therefore, a high master current overshoot can be achieved during the start-up transients since the master has no current control [15]. Communication signals of relatively high bandwidth, i.e., instantaneous current and voltages, are distributed throughout the system.

Different strategies for assigning the master are possible, such as [16]:

- dedicated: master is a fixed module
- rotary: master is arbitrarily chosen
- highest-crest current: master is the module with maximum rms or crest current

With both configurations, the reliability of the power system is dedicated to a large extent by the reliability of the master unit [18]. Therefore, in [18], a rotating priority window, providing random selection of the master is suggested to increase the reliability. In [19], extended monitoring by two redundant monitoring systems is performed. These systems define one of the healthy blocks as the master.

4.2.1. *Without central controller*

The master/slave control scheme without central controller consists of a single master and a set of slave inverters without additional central controller [15,13,16,17]. The master operates as a voltage-source inverter (VSI) in order to control the load voltage as shown in Fig. 3. It also measures the total load current and determines the set-value of the current for each slave unit. The slave units operate in current-control mode acting as current-source inverters (CSIs). In the master/slave control method of Fig. 3, derived from its dc/dc variant in [15], the reference current of the slaves equals the master output current $i_m = i_{ref}$. A current controller controls the slaves' output current $i_{L,i}$ to the reference current i_{ref}. The output of the slave's current controller v_c is added to a master-signal v_e and forms the input of the PWM. The signal v_e can be seen as a feed-forward term. The master module controls v_0 to v_{ref} via a voltage controller with output v_e, which is directly used for the PWM pulse generation of the master.

An advantage of this strategy is that voltage recovery is obtained by the voltage controller of the master and the current control loops of the slaves together [13]. A disadvantage is that both current sharing signals (i_m) and voltage (v_e) feedback signals are distributed by using a relatively high bandwidth communication link as instantaneous values are communicated [13]. The current sharing is accurate in steady-state, but during the transients, large differences between master and slave currents can occur due to the limited bandwidth of the communication. The master delivers most of the compensation current.

For the master/slave communication scheme, several possibilities exist. In a first one, the master unit sends its signals to all other units. Therefore, the number of interconnections in this implementation can become quite large. However, if any slave fails, the system would still be operational, leading to a certain degree of redundancy. In a second implementation, the units are arranged in ring configuration. Therefore, the master unit sends its signals only to one (first) or two (first and last) slave units. This reduces the number of interconnections, but can compromise the redundancy.

4.2.2. *With central controller*

A second variant on master/slave control is the control strategy with a central controller as shown in Fig. 4. This approach is based on the method for operating UPS systems in parallel and is described in [13,9,20–22]. The master is responsible for the voltage control and is, thus, a VSI, while the slaves take care of the current control in the CSI mode. Opposed to the control method without central controller, the master current is not equal to the reference current and the master does not provide this reference current to the slave units any more. This task is performed by a central control unit, that calculates the central-limit reference current ($i_{ref} = i_{load}/N$) and distributes this to all slave units. Compared to the method without central controller, the voltage reference value is not shared, the only distributed signal is the slaves' reference current i_{ref}.

The advantages and disadvantages are analogous to those of the master/slave control without central controller. Like in the previous master/slave control during transients, the master tries to recover the output voltage, which may lead to large master current transients [13]. This can become critical in large systems wherein the master has to take the transients of the whole system. Only one signal has to be distributed, but still a high bandwidth of the communication link is required. There is always a time or phase delay between the output current of each slave unit and the load current [9].

An advantage of this method is that in grid-connected mode the grid can be regarded as the master. Therefore, there is no need for specific control methods for grid-connected and islanded operation. Also, good load sharing is achieved. However, because of the presence of a single central controller and one master, the system is not redundant.

4.2.3. *Auto-master–slave control*

In [23], an auto-master–slave control strategy is proposed, which is a variant of the master/slave control. The main principle is depicted in Fig. 5.

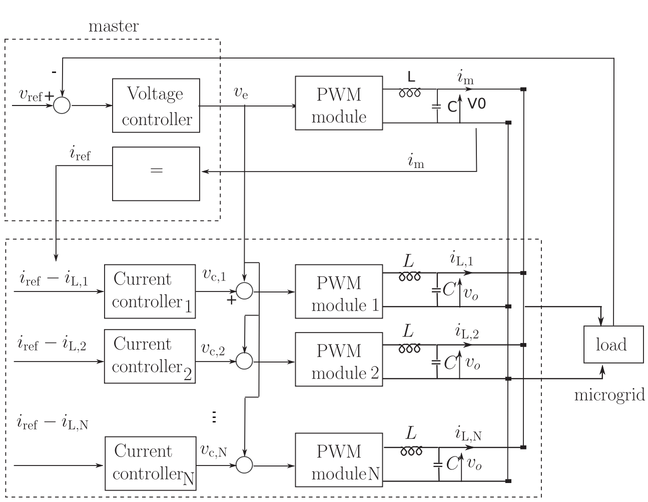

Fig. 3. Master/slave control principle without central controller.

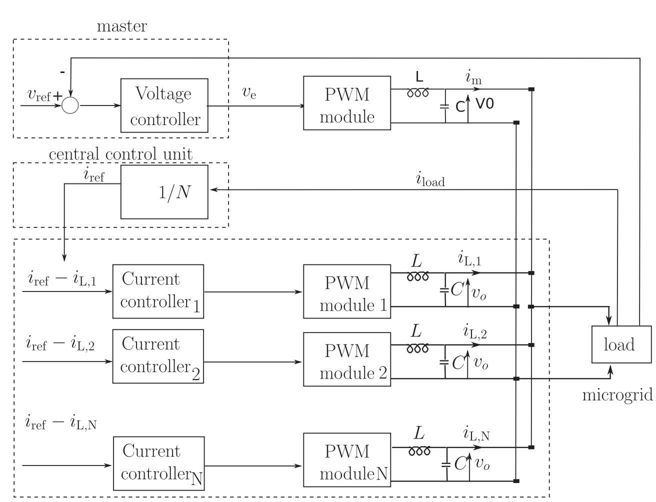

Fig. 4. Master/slave control principle with central controller.

The control circuitry employs an active power share bus and a reactive power share communication bus interconnecting all the paralleled units [23]. All inverters measure their output power. The inverter with the highest output power becomes the master inverter, drives the power bus and its power is the reference for the other inverters [23]. Although two buses are used in this method, the signals are almost dc and the noise can be eliminated easily, so the information can be transferred over long distances [23]. This is in contrast to the master/slave and central control schemes, where instantaneous values of voltage and/or current (i.e., varying with at least a 50 Hz frequency) need to be distributed. The master of real power drives P_{bus}, which becomes the reference signal for the other units. In the master, $\Delta P=0$, while for the slaves $\Delta P=P_{bus}-P_i$. By using ΔP, the frequency compensation value is calculated. Therefore, the master works in reference frequency $f=f_{ref}$. For the reactive power, an analogous regulation is adopted in [23], also including a master reactive power unit. The value ΔQ determines the reference voltage of the units.

4.3. Instantaneous(-average) current sharing

Another control strategy that depends on inter-unit communication is the instantaneous current sharing technique. Opposed to the master/slave control scheme, no master controller is present. Average current sharing does require a current sharing bus and reference synchronization for the voltage. The voltage and current references are the shared signals among the modules. The objective of the shared information is to determine the deviation of the individual output current from the desired value [24]. Since the output currents of the inverters are regulated at every switching cycle, the instantaneous-current sharing scheme has a good performance both on current sharing and voltage regulation [24]. Even if the output currents contain many harmonics, the inverters can share the output currents equally. However, interconnections between the inverters are necessary. This limits the flexibility of the system and degrades the redundancy [24].

The control principle is depicted in Fig. 6. Each inverter is connected to the load through an impedance Z_i. By taking this impedance into account, there is no common voltage reference of the DG units equal to the load voltage v_o. The references of the voltage-feedback loops are synchronized to make the output voltages of all inverters in phase. To achieve this, a common voltage reference is generated for all the individual modules [25]. This voltage reference is the input of the inner voltage control loop. The output of the outer current-sharing loop is added to this

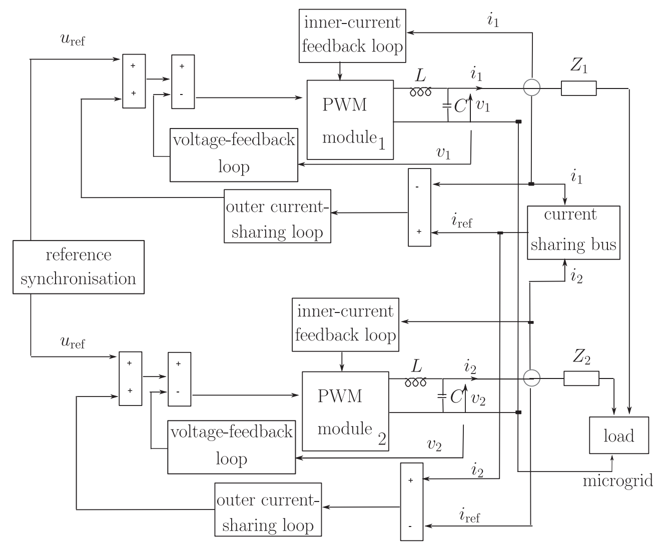

Fig. 6. Instantaneous average current sharing.

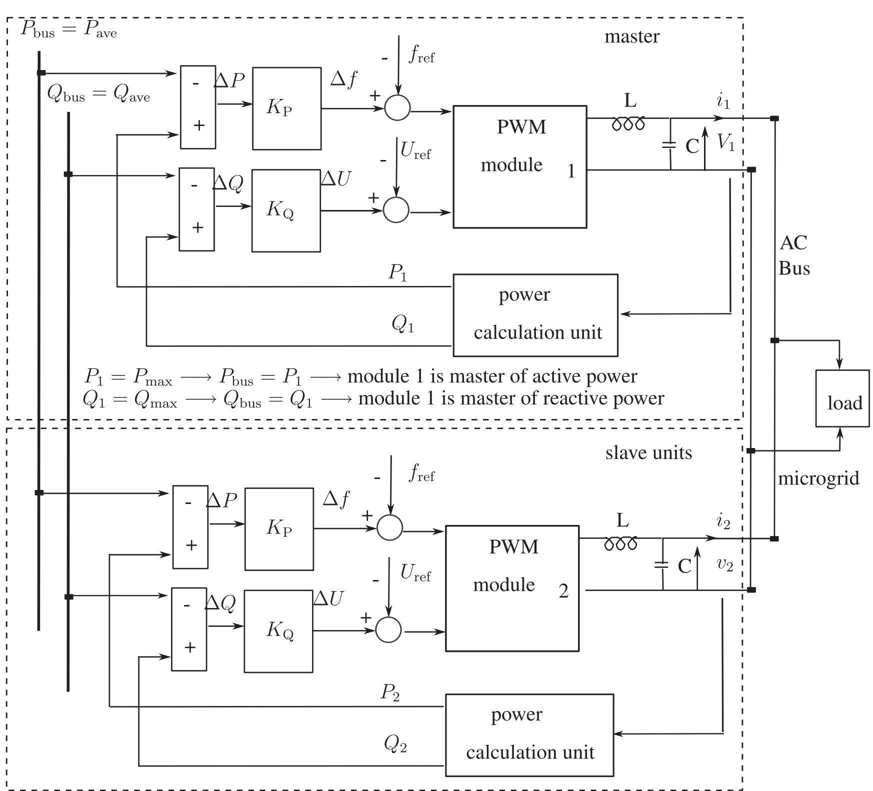

Fig. 5. Auto-master–slave control principle.

value such that each inverter contributes the same power to the load [24]. Each inverter provides a measurement of its output power to the current-sharing bus, which generates a common current reference i_{ref} [24,26]. The value i_{ref} minus the measured terminal current of the DG units forms the input of the current sharing loop.

The reference i_{ref} can be the highest output current, the output current of the inverter with the highest clock frequency or the averaged output current [24]. A disadvantage of the highest current control (HCC) is that the sensed highest output current can include noise, which deteriorates the performance of the current distribution and output voltage regulation. In addition, non-identical component characteristics and input voltage variation of the paralleled inverters might also deteriorate in system performance [27]. In [27,28], the averaged current-sharing strategy (ACSS) is used to achieve an equal current distribution and to reduce noise effects occurring at the converter switching transition. In [29], the average current sharing method is combined with load current feed-forward to improve the output characteristics. However, with the HCC and ACSS, it is difficult to achieve a weighted current distribution control when the paralleled inverters have different power ratings [30]. Therefore, a current-weighting-distribution-control (CWDC) is used in [30] to achieve a weighted output current distribution among the inverters. This allows for inverters with different power ratings, opposed to the case where the factor $1/N$ is used for the current distribution. The control strategy is analogous to the other instantaneous current sharing strategies and is depicted in Fig. 7. First, the average current is calculated, which is defined as (with N the number of units)

$$i_s = \frac{\sum_{i=1}^{N} i_{L,i}}{N} \tag{1}$$

Then, for each unit, the reference current is calculated by using a weighting function:

$$i_{ref,i} = i_s \frac{P_i}{(\sum_{i=1}^{N} P_i)/N} \tag{2}$$

The value P_i represents the nominal active power output of inverter i.

To improve the current and power sharing when the line impedance is different among the inverters, adaptive gain scheduling is introduced in the instantaneous average current sharing control scheme in [26].

4.4. Peak-value based current sharing

In [31,32], the control area network communication protocol is used to obtain accurate power sharing and smooth mode transfer. In the islanded microgrid operating condition, one converter operates with a voltage dual-loop controller to control the ac-bus voltage to a reference value. For this, an inner current control and an outer voltage control loop with proportional-resonant (PR) controllers are used. The other converters only have a current control loop with a PR controller. The control strategy is summarized in Fig. 8. The reference amplitude of the current-controlled inverters is determined by the obtained current amplitude of the voltage-controlled inverter by using peak value calculation (PC) and is communicated via a communication bus [32]. The reference phase is determined by using a PLL that calculates the phase angle of the voltage of this module. An automatic reference generation (ARG) calculates the current reference of the current-controlled units, to minimize the current peak difference and phase difference. Only the magnitude and phase information of the ac current need to be communicated [32]. The frequency

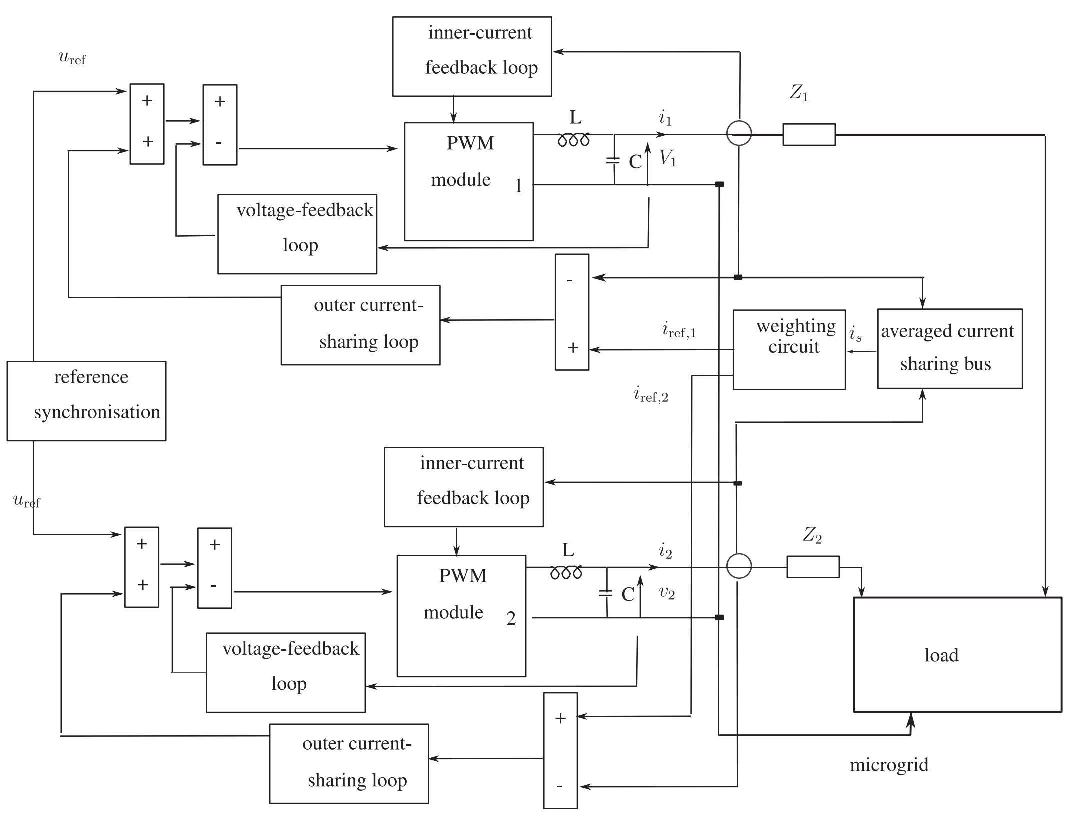

Fig. 7. Current-weighting-distribution-control.

information is not transmitted because it is automatically tracked by the PLL (opposed to the master/slave control scheme).

4.5. Circular chain control

In the circular chain control (3C) scheme depicted in Fig. 9, the modules are connected in a circular configuration and each module tracks the inductor current of the previous one. In this way, equal current distribution is achieved [33]. An outer voltage control loop is used, such that each module controls its output voltage v_o to a reference value v_{ref}. As shown in Fig. 9, line impedances are neglected, thus, a small system is considered. The output of the voltage controller, together with the measured inductor current of the module and that of the subsequent one, forms the input of the inner current control loop.

4.6. Distributed Control

The distributed control method can be applied to parallel converters [13,34]. It is important in distributed control to reduce the number of communication lines to improve the implementation and the reliability. The shared bus consists of signals such as voltage reference, current reference and averaged feedback voltage, which come from all the modules. In this way, the system will keep running in case a module breaks down.

The distributed control method (DCM) of [13] uses low-bandwidth communication to maintain instantaneous power sharing and high power quality under various loads. In the previous methods, if the bandwidth of the distributed signals decreases, the disturbance rejection will be compromised as higher frequency components are not regulated. Therefore, in the DCM method, a central controller provides fundamental frequency power sharing between the different converters by distributing a low-bandwidth signal to all converters. Power quality aspects are dealt within the local controllers, by means of higher-frequency signals. The difference between the conventional control schemes and the DCM method of [13] is shown in Fig. 10, with d a disturbance. In the conventional control scheme, a signal y is controlled to its reference value $y^{\star}$, with controller output $v^{\star}$. In the DCM, a remote central controller regulates the low-frequency components of y,

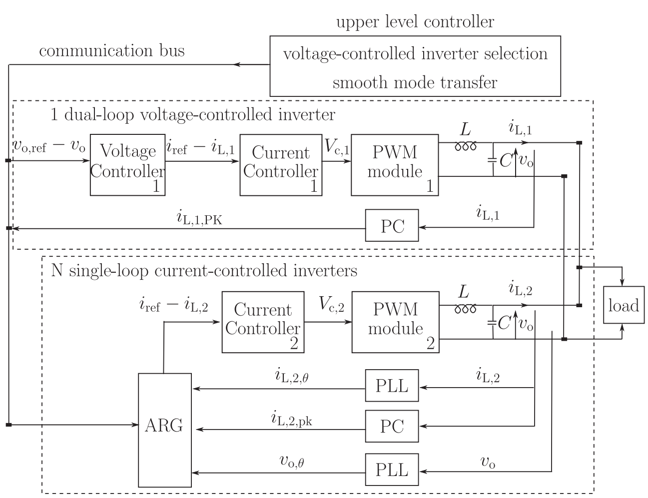

Fig. 8. Peak-value based current sharing (pk=peak value; θ=phase angle).

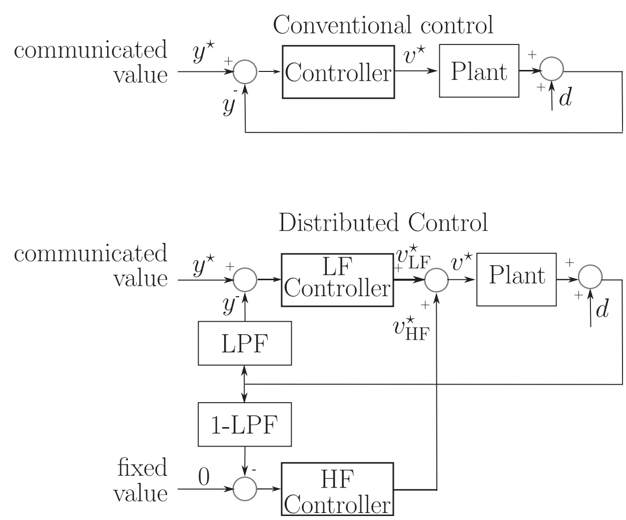

Fig. 10. Conventional control scheme versus distributed control scheme.

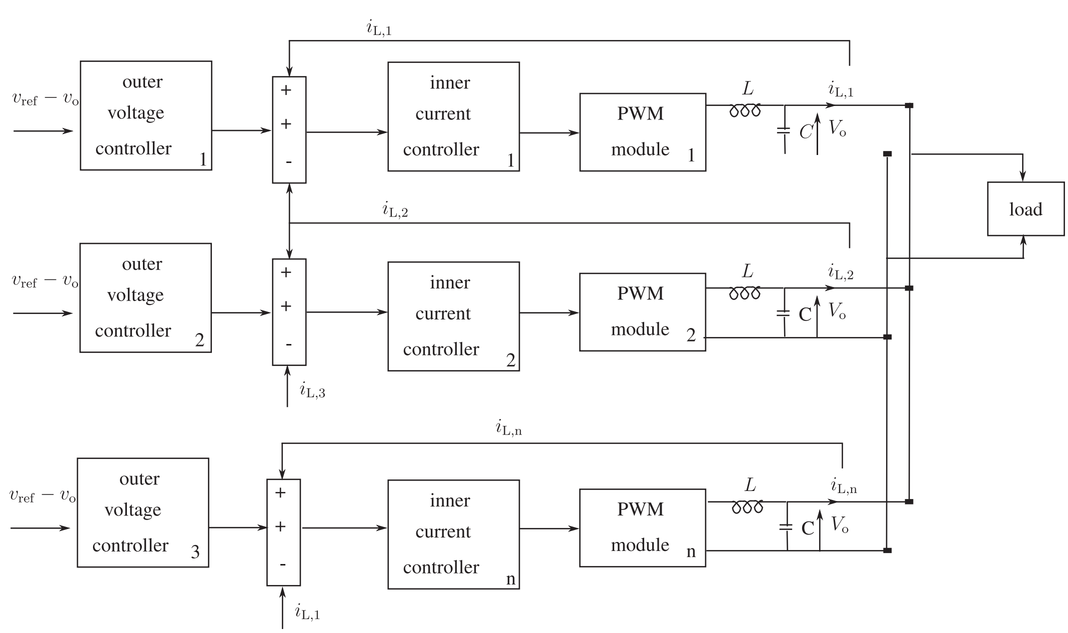

Fig. 9. Circular chain control.

determining $v^{\star}_{\mathrm{LF}}$ and communicating it to the plant by means of a low-bandwidth signal. For the higher frequency components, a high-bandwidth signal is locally controlled to zero.

The DCM scheme is shown in Fig. 11. The central controller controls the low-frequency components of the load voltage to V_{ref} and determines the low-frequency reference $i^{\star}_{\mathrm{L,LF}}$ for the converters, that has relatively low bandwidth and can be transmitted via a communication link of limited bandwidth [13,34]. Steady-state and low-frequency issues are, thus, controlled centrally and a low-bandwidth communication channel is employed to distribute the control signals to the individual units. The control is distributed between this low-bandwidth central controller and high-bandwidth local controllers. The local controllers are responsible for rejecting high-frequency disturbances, such as harmonic suppression, without the use of a communication channel [13,34]. They control the high-frequency components of the load voltage to zero. The current controller's input is formed out of three components. The first component consists of the central $i^{\star}_{\mathrm{L,LF}}$ for fundamental frequency power sharing and voltage regulation. The second input of the current controller is the local voltage controller's output, which determines the high-frequency component feedforward of the inverters output current $i_{\mathrm{L,i,HF}}$ and leads to additional power quality improvement. The third is the measured high-frequency component of the output current.

In conclusion, voltage regulation and fundamental power sharing are controlled centrally. The DCM method is distributed in the sense that the higher frequency components are dealt with by local controllers. However, still, a single point of failure is present. The supply of harmonic currents to the loads and disturbance rejection requires a high-bandwidth feedback and is handled locally by each inverter [13,34]. The main advantage of the method proposed in [13,34] is that the control topology uses a communication link of limited bandwidth to maintain power sharing between the units.

The distributed control can be seen as a variant on the master/slave control. A central control block controls the reference voltage and influences the output current of the units. The voltage magnitude, frequency and power sharing are centrally controlled. Hence, in distributed control, only low bandwidth communication is required. The harmonic support is done locally, opposed to in the master/slave control scheme.

4.7. Angle droop

In [35], angle droop control is presented. This is a control method that uses communication for phase angle referencing. In the conventional droop methods, which are discussed further, P and Q are controlled through the frequency and amplitude of the reference voltage. In angle droop control, the phase angle, relative to a system-wide common reference (a phase angle reference), is used for the control:

$$\delta = \delta_0 - m(P - P_0) \tag{3}$$

$$V = V_0 - n(Q - Q_0) \tag{4}$$

Mostly, GPS signals are used to obtain the reference angle. In this way, no inter-unit communication is required. In [35], it is discussed that the choice for using phase angle instead of frequency in the active power droop is beneficial as the maximum frequency restricts the choice of droop gain in the conventional P/f droop control. This can lead to chattering in case of frequent load changes [35].

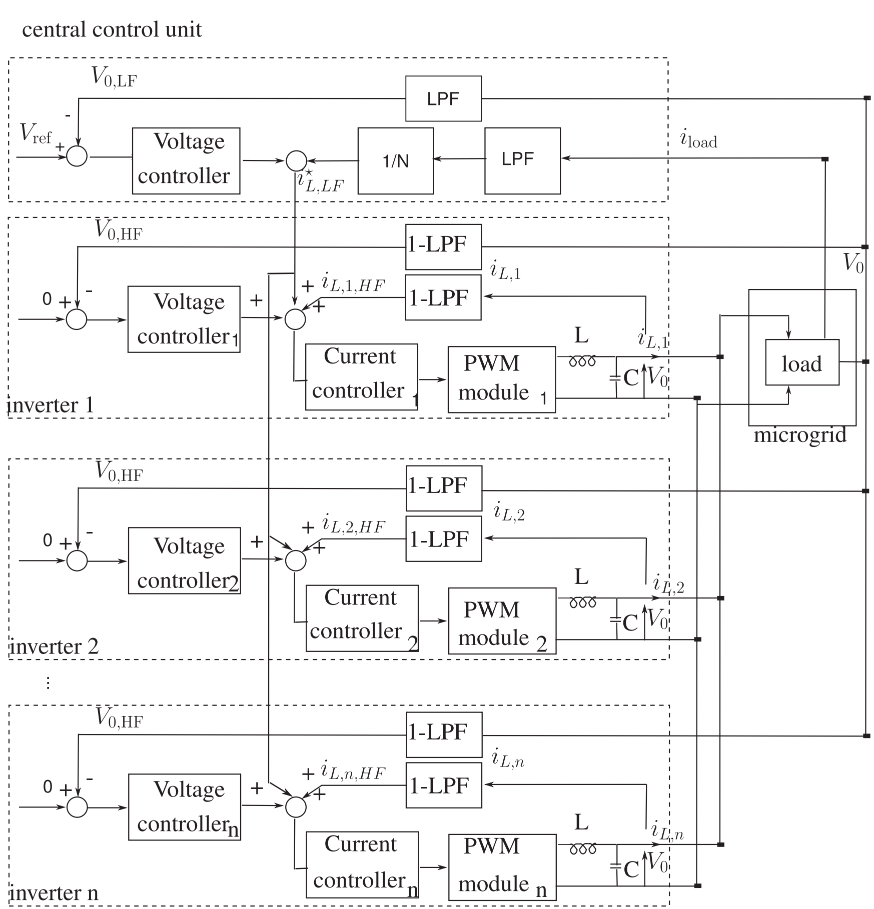

Fig. 11. Distributed control method (HF=high-frequency, LF=low-frequency).

5. Control strategies without communication

The strategies that operate without inter-unit communication for the primary control are based on droop control. Operation without a communication link is often essential when connecting remote inverters. It also makes it easy to achieve redundancy and avoids the complexity, high costs and the requirement of high reliability of a supervisory system. Also, such systems are more easy to expand because of the plug and play features of the modules. Therefore, especially for long distances and high-bandwidth requirements, communication lines are often avoided. Nevertheless, droop control also has some inherent drawbacks, such as the trade-off between power sharing accuracy and voltage deviations, unbalance in harmonic current sharing and dependency on the inverter output impedance. To overcome these issues, some variations on the conventional droop controllers have been presented, such as injecting high-frequency signals (i.e., > 50 or 60 Hz) in the power lines as discussed in Section 5.3. Another disadvantage is that the local controllers in the converters are more complex than when a central controller is used [8].

Here, only primary controllers are considered. Overlaying secondary and tertiary controllers can change the set-points of the primary controllers by using communication. The primary objective of the primary controller is to maintain the stability of the system [36].

5.1. P/f droop control

A well-known way to realize a plug and play feature for each DG unit is employing the conventional droop control [2]. In the transmission system, the synchronous generators are equipped with P/f droops. If the extracted ac power of the power station is larger than its input mechanical power, the generator will slow down because of its inertia. Hence, the frequency of its terminal voltage will lower. In this way, the phase angle of the voltage will decrease and because of the line characteristics, also the ac power will decrease. In this way, a self-regulating system is obtained [37]. The frequency is a global parameter, i.e., equal (constant) in the entire system and the rotational speed of the generators is directly linked to the frequency. Hence, each generator will measure its speed and droops it in a P/f droop with negative slope to change its input mechanical power. In this way, accurate power sharing between different generators is obtained.

5.1.1. Conventional P/f droop control

Droop control was introduced for standalone microgrid control in [1,36,38–43]. The P/f droop control method is based on mimicking the operation of synchronous generators. In the conventional power system, the droop control method changes P as a function of the grid frequency, and is based on the inertia of the synchronous machines ($P(f)$). As the converter-based microgrids generally lack this inertia, the P/f droop method in microgrids is based on the line characteristics as discussed below. The power flow equations from a source E_1 with phase angle δ to a voltage E_2 with phase angle 0 (phase angles are relative values) through a line impedance $Z = R + jX$ equal:

$$P = \frac{E_1}{R^2 + X^2}[R(E_1 - E_2 \cos\delta) + XE_2 \sin\delta] \tag{5}$$

$$Q = \frac{E_1}{R^2 + X^2}[-RE_2 \sin\delta + X(E_1 - E_2 \cos\delta)] \tag{6}$$

For a mainly inductive line impedance, R may be neglected. Further considering that δ is typically small, it is reasonable to assume that $\sin\delta \approx \delta$ and $\cos\delta \approx 1$ [2]:

$$P \approx \frac{E_1}{X}[E_2\delta] \tag{7}$$

$$Q \approx \frac{E_1}{X}[E_1 - E_2] \tag{8}$$

For this reason, in inductive networks, a linkage between active power and phase angle δ and between reactive power and voltage amplitude exists. For the control, the frequency is used instead of the phase angle as the units do not know the initial phase value of the other units. Also, due to component tolerances for example, minor differences in the frequency of a signal can occur although the same reference frequency is used. Hence, it is necessary to compensate for the difference between the crystal clock generators [16]. Therefore, in the P/f droop control method, the P of the generators is drooped with the measured terminal frequency ($P(f)$). However, in converter-based microgrids, measurements of the instantaneous frequency are not straightforward, while measuring the active power is easier [40]. On the other hand, the frequency of a converter-system can be controlled independently, opposed to the frequency of a synchronous generator that is linked to its rotational speed. Therefore, generally, a droop with f as a function of the measured P ($f(P)$) is proposed, which is analogous to determining P as a function of the measured f ($P(f)$) [44]

$$\omega_i = \omega_{\mathrm{ref}} + K_{\mathrm{P}}(P_i - P_{\mathrm{i,ref}}) \tag{9}$$

Preferably, the droops are coordinated to make each DG system supplying real power in proportion to its power capacity [2]

$$K_{\mathrm{P}} = \frac{\omega_{\mathrm{ref}} - \omega_{\min}}{P_{\mathrm{i,ref}} - P_{\mathrm{i,max}}} < 0 \tag{10}$$

In case multiple DG units are connected in parallel, they share the load according to their droops analogously as in the conventional power system. Similarly, the amplitude of the voltage is drooped with the measured reactive power

$$V_i = V_{\mathrm{ref}} + K_{\mathrm{Q}}(Q_i - Q_{\mathrm{i,ref}}) \tag{11}$$

$$K_{\mathrm{Q}} = \frac{V_{\mathrm{ref}} - V_{\min}}{Q_{\mathrm{i,ref}} - Q_{\mathrm{i,max}}} < 0 \tag{12}$$

The choice of K_{P} and K_{Q} influences the network stability [45].

The control algorithm with conventional droop control is depicted in Fig. 12. The invertor operates as a voltage source with voltage and frequency determined by local control loops [36]. Only the steady-state power and voltage are communicated by using secondary controllers in a microgrid management scheme. An advantage of the droop method is its simplicity because no extra interconnections among the inverters are required. Therefore, high modularity, flexibility (i.e., plug and play) and good reliability can be achieved. However, the performance of the voltage regulation and the transient responses is lower and the harmonic currents cannot be shared properly with the conventional P/f droop control method. Also, there is an inherent trade-off between voltage control against the accuracy of Q and P sharing [46,47]. In choosing the droop coefficients, there is a trade-off between the magnitude of the droop and the stability. Large droops speed up the load sharing, but can cause instability. Smaller droops slow down the control [37]. Because of the proportional controllers without integral term (i.e., droops), the frequency and voltage in the microgrid are not constant but load-dependent . A slow dynamic response is obtained as low-pass filters are required to calculate the average P and Q [46]. Another disadvantage of this method is the inability to provide rejection of the voltage harmonic content and to control zero-sequence unbalance [34].

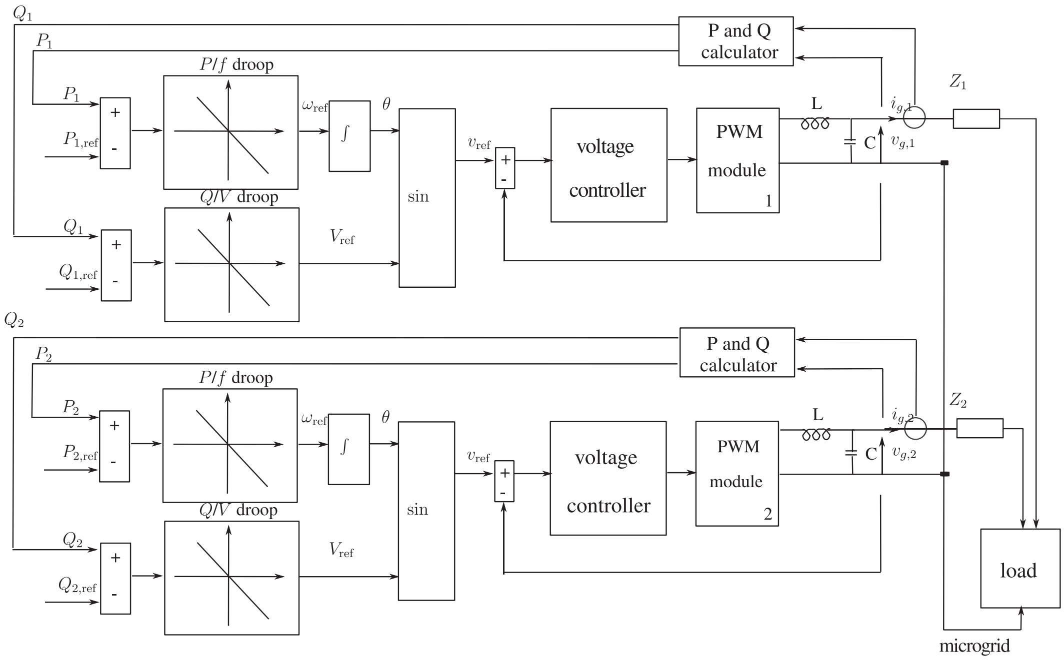

Fig. 12. Conventional droop control: P/f droops and Q/V droops.

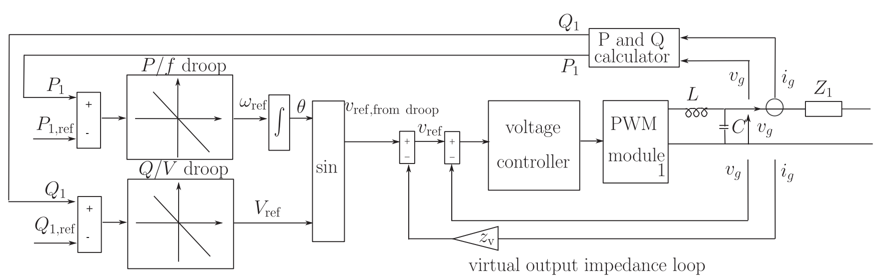

Fig. 13. P/f droops and Q/V droops with virtual output impedance.

Some solutions to these issues have been discussed in the literature. A virtual output impedance [48], frequency restoration [49] and a derivative controller [50–52] can be included in the droop method.

5.1.2. Variants on P/f droop control

The droop control method has some problems to be solved, like a line-impedance dependency, inaccurate P or Q regulation and slow transient response [53]. Therefore, different variants on P/f droop control have been presented to cope with these issues.

Derivative term. To improve the dynamics of the system, a derivative term is included in the adaptive derivative droop in [51]:

$$\omega = \omega^{\star} + K_{\mathrm{P}}(P_i - P_{\mathrm{i,ref}}) + K_{P,d}\frac{dP_i}{dt} \tag{13}$$

$$V_i = V_{\mathrm{ref}} + K_{\mathrm{Q}}(Q_i - Q_{\mathrm{i,ref}}) + K_{Q,d}\frac{dQ_i}{dt} \tag{14}$$

In small microgrids, large load changes can be expected, hence, adaptive transient derivative droops ($\hat{}$ -values) are used in [51] to add damping and to avoid large start-up transients and circulating currents

$$\omega = \omega^{\star} + K_{\mathrm{P}}(P_i - P_{\mathrm{i,ref}}) + \hat{K}_{P,d}\frac{dP_i}{dt} \tag{15}$$

$$V_i = V_{\mathrm{ref}} + K_{\mathrm{Q}}(Q_i - Q_{\mathrm{i,ref}}) + \hat{K}_{Q,d}\frac{dQ_i}{dt} \tag{16}$$

A pole placement problem changes $\hat{K}_{P,d}$ and $\hat{K}_{Q,d}$ [51].

Virtual output impedance. To avoid P–Q coupling, a virtual output inductor can be included, which introduces a predominantly inductive impedance without the need for line impedance information. In [48,50], a virtual inductive output impedance is implemented in the inverter by including fast control loops in the droop control method as shown in Fig. 13. The input of the voltage controller becomes [2]:

$$v_{\mathrm{ref}} = v_{\mathrm{ref,from\ droops}} - L_{\mathrm{virt}}\frac{di_{\mathrm{g}}}{dt} \tag{17}$$

A concern from the virtual inductor control scheme is the derivation of line current i_{g} [2]. Differentiation can cause high-frequency noise amplification, which in turn may destabilize the DG voltage control scheme especially during a transient [2]. A common approach to avoid noise amplification is to add a low-pass filter to the measured grid current to avoid the introduction of excessive noise into the system [54,2,46]. However, this approach is subject to the trade-off between the high frequency noise attenuation and the fundamental component phase and gain errors (or tradeoff between the overall control scheme stability and the virtual inductor control accuracy) [2]. Therefore, another method is using a high-pass filter instead of

a pure derivative [48]

$$v_{\mathrm{ref}} = v_{\mathrm{ref,from\ PQ\ droops}} - \frac{s}{s+\omega_C} L_{\mathrm{virt}} i_g \tag{18}$$

The virtual output impedance method is effective in preventing the P–Q coupling, but can increase the reactive power sharing error due to increased voltage drops. Therefore, in [2], the reactive power control is improved by on-line estimating the voltage drops and the local load demand.

In addition, soft start is included in [46] to avoid initial current peaks

$$L_{\mathrm{virt}} = L^{\star}_{\mathrm{virt,f}} + (L^{\star}_{\mathrm{virt,0}} - L^{\star}_{\mathrm{virt,f}}) e^{-t/T_{\mathrm{start}}} \tag{19}$$

with $L^{\star}_{\mathrm{virt,0}}$ and $L^{\star}_{\mathrm{virt,f}}$ the initial and final values of the virtual output impedance and T_{start} the time constant of the soft start operation.

Frame transformation. To avoid P/Q coupling, next to the virtual output impedance method, virtual P and Q frame transformation has been proposed [55]. A transformation matrix with angle θ, that is dependent on the R/X value of the lines, is used to calculate the virtual powers P' and Q'. The droops become:

$$\omega_i = \omega_{\mathrm{ref}} + K_P (P'_i - P'_{i,\mathrm{ref}}) \tag{20}$$

This is equal to

$$\omega_i = \omega_{\mathrm{ref}} + K_P \frac{X}{Z} (P_i - P_{i,\mathrm{ref}}) + K_P \frac{R}{Z} (Q_i - Q_{i,\mathrm{ref}}) \tag{21}$$

For the reactive power

$$\begin{aligned} V_i &= V_{\mathrm{ref}} + K_Q (Q'_i - Q'_{i,\mathrm{ref}}) \\ &= E_{\mathrm{ref}} + K_Q \frac{X}{Z} (Q_i - Q_{i,\mathrm{ref}}) + K_Q \frac{R}{Z} (P_i - P_{i,\mathrm{ref}}) \end{aligned} \tag{22}$$

The droops are, thus, equal to those of (9) and (11), but with P and Q replaced by P' and Q', respectively. In this way, despite the non-zero R/X value of the lines, P/Q decoupling is achieved as if the network were purely inductive. In general, the value X/R is not accurately known, but according to [55], an estimation of R/X is sufficient.

Another method that uses frame transformation is presented in [56]. Here, the transformation angle θ is continually adapted to reach a minimum current and accurate power sharing. However, according to [57], the slow dynamics of the added current droop can make this method impractical.

As the virtual power frame ($P'-Q'$) cannot directly and accurately share the actual power, in [58,59], a virtual frequency–voltage ($\omega'-E'$) frame is used. This method also achieves a decoupled power control and an improved system stability.

In [60], an adaptive droop controller is presented in which the grids phase angle is estimated by using a PLL to determine the frame transformation angle θ.

Harmonic power sharing. An interesting method to share the harmonic burden is the usage of G/H droops, with G the harmonic conductance and H the harmonic var (volt–ampere reactive), in [61] and shown in Fig. 14. The harmonic power H is calculated according to the instantaneous reactive power theory [62]. This method is based on inductive lines, thus the G–H droop control cooperates with P–f and Q–V droop controllers for the fundamental components.

In [63], a variant of these G/H droops is presented. The distortion D is calculated by using $S^2 = P^2 + Q^2 + D^2$. The distortion is shared by adopting the gain (and bandwidth) of the voltage controller dependent on D as shown in Fig. 15. The downside is a reduction in voltage waveform quality.

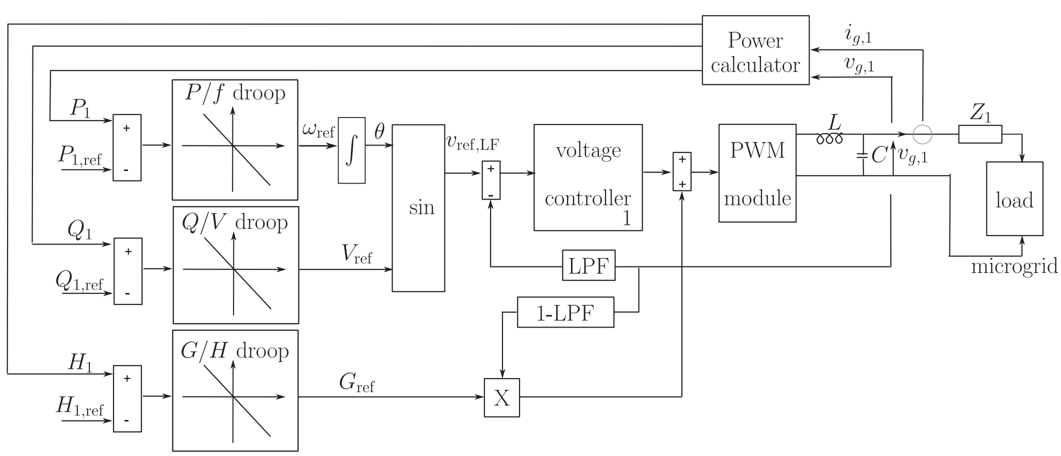

Fig. 14. Harmonic power sharing: P/f, Q/V and G/H droops.

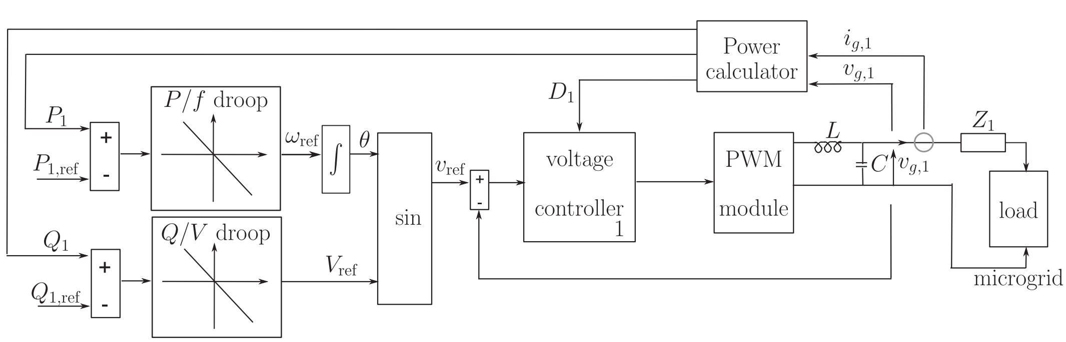

Fig. 15. Harmonic power sharing: sharing the distortion by adapting the bandwidth of the voltage controller.

In [46], an additional current harmonic loop is added in the control strategy for properly sharing non-linear loads. Selective harmonic current sharing is used to treat the significant output-current harmonics separately by using bandpass filters.

Virtual inertia: In normal operating conditions, the frequency is limited by the narrow margins of the primary controllers, the presence of rotating inertia in the system and the frequency-dependent consumption of, e.g., electrical motors. The primary control stabilizes the frequency after an event, but has no significant effect on the initial frequency deviations. As the number of generators and loads that are not directly coupled to the network is steadily increasing, the available inertia decreases (certainly in islanded microgrids) [64]. This decreased inertia results in faster and larger frequency deviations after an event, which may cause problems in the network [65–70]. To emulate rotating inertia, the DG units can be operated as virtual synchronous generators (VSGs). VSGs require additional reserve, which enables them to damp initial transients and stabilize the system. The additional control power can support the frequency stability even before the primary reserve is activated, hence, contributes to the pre-primary reserve of the microgrid. Different variants of a VSG exist, such as VSGs based on frequency measurements in [65,66], VSGs based on power measurements in [67,71] and synchronverters in [70,72].

5.2. P/V droop control

Low-voltage networks are mainly resistive, leading to the usage of P/V droop controllers. A disadvantage of this method is that the compatibility with the large central generators can be lost if the DG units need to contribute in the load sharing evenly with the synchronous generators. However, islanded operation is considered here. The advantage is that there is a better match between the control strategies and the characteristics of the considered networks, such as the lack of rotating inertia, resistive lines and high share of renewable sources.

5.2.1. P/V droop control

While the P/f droop control method works well in a power grid with mainly inductive line impedances, it leads to a concern when implemented on a low-voltage microgrid, where the feeder impedance is not inductive and the line resistance should not be neglected [2]. This is especially true for DG units without grid-side inductor or transformer, where the output inductance is very small [2]. In case of mainly resistive lines, the power flow equations become:

$$P \approx \frac{E_1}{R}[E_1 - E_2] \tag{23}$$

$$Q \approx \frac{E_1}{R}[-E_2\delta] \tag{24}$$

Hence, the active power is mainly linked with the voltage difference, while reactive power is mainly linked with the phase angle, hence frequency. This leads to P/V and Q/f droops as opposed to the conventional P/f and Q/V droops [7,40,73–75]. The active and reactive power is measured and drooped to obtain the rms voltage and its frequency respectively

$$V_i = V_{\mathrm{ref}} + K_{\mathrm{P}}(P_{\mathrm{i,ref}} - P_i) \tag{25}$$

$$\omega_i = \omega_{\mathrm{ref}} + K_{\mathrm{Q}}(Q_{\mathrm{i,ref}} - Q_i) \tag{26}$$

with $K_P < 0$ and $K_Q > 0$. The control scheme is depicted in Fig. 16.

In [75], the P/V droops are compared with the P/f droops. It is concluded that the former are better in resistive networks as they give a more damped response.

5.2.2. Variants on P/V droop control

Virtual output impedance: A resistive virtual output impedance can be enforced by subtracting a proportional term of the output current from the reference voltage [50]

$$v_{\mathrm{ref}} = v_{\mathrm{ref,from\ droops}} - i_g R_v \tag{27}$$

The main advantages are: P/Q decoupling, an enhanced stability and dynamic response of the studied system (a more damped system) [50,53].

In [76], this is extended with G–H droops in combination with P–V and Q–f droops.

Voltage-based droop control: In voltage-based droop (VBD) control strategy of [77], the P/V droop controller is divided into two droop controllers and constant-power bands are included as depicted in Fig. 17. In a VSI, the dc-link voltage V_{dc} automatically shows changes in the ac or dc power. A V_g/V_{dc} droop controller is used to enable power balancing between the ac and dc-side of the

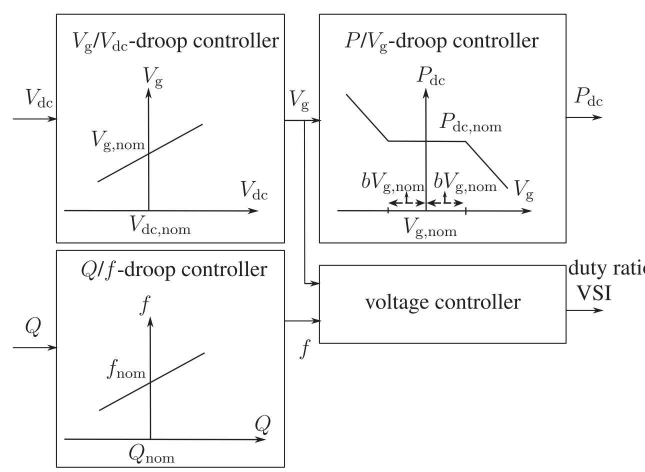

Fig. 17. VBD control: droops to obtain the reference voltage.

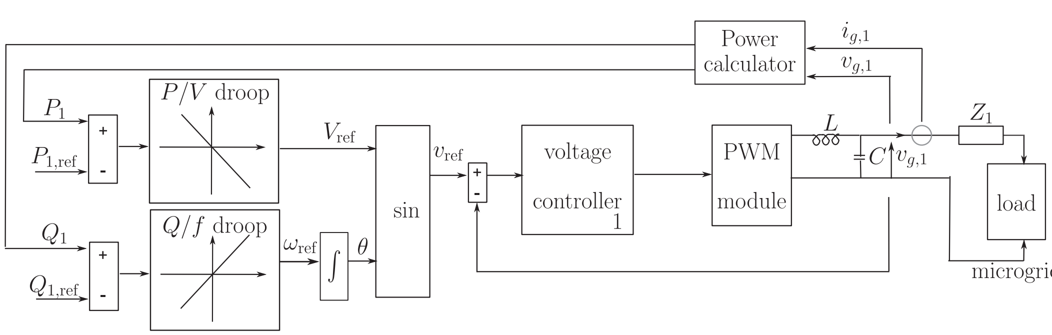

Fig. 16. *P/V* droop control: *P/V* droops and *Q/f* droops.

VSI:

$$V_g = V_{g,\text{ref}} + K_V(V_{dc} - V_{dc,\text{ref}}) \tag{28}$$

with $K_V > 0$. In order to also include voltage limiting, P_{dc}/V_g droops are used. A dead-band is included, which is called the constant-power band

$$P_{dc} = \begin{cases} P_{dc,\text{nom}} - K_p(V_g - (1+b)V_{g,\text{nom}}) \\ \quad \text{if } V_g > (1+b)V_{g,\text{nom}} \\ P_{dc,\text{nom}} \\ \quad \text{if } (1-b)V_{g,\text{nom}} < V_g < (1+b)V_{g,\text{nom}} \\ P_{dc,\text{nom}} - K_p(V_g - (1-b)V_{g,\text{nom}}) \\ \quad \text{if } V_g < (1-b)V_{g,\text{nom}} \end{cases} \tag{29}$$

The width $2b$ of this band is dependent on the nature of the source as shown in Fig. 18. Dispatchable DG units have small constant-power bands to fully take advantage of their power control capabilities. The less dispatchable units, such as renewables, also contribute in the power sharing and balancing, but have a large band. Hence, changing the input power of these units is only required for large deviations from the grid voltage to its nominal value. The overall control scheme is depicted in Fig. 19.

Note that the conventional P/V droop of Fig. 16 also requires an additional controller for the dc-link balancing, which is achieved by the V_g/V_{dc} droop controller in the VBD control scheme.

In [75], a dead band around the nominal voltage and frequency is used as well. This dead band prevents control actions for each V_g and f deviation, which may lead to stability problems such as oscillations in the system [75].

In [78], an additional loop is included in the VBD control strategy to ensure controllable harmonic power sharing.

Derivative term: To also improve the dynamics of the system, a derivative term is included in [50]

$$V_i = V_{\text{ref}} - nP - n_d \frac{dP}{dt} \tag{30}$$

$$\omega_i = \omega_{\text{ref}} + mQ + m_d \frac{dQ}{dt} \tag{31}$$

The controller does not include integrating terms as this would induce an unstable system [50].

5.3. Frequency-based signal injection

Several current sharing techniques based on frequency encoding of the current-sharing information have been presented. The network lines are used for the communication for the power sharing (power-line communication). This method has significant advantages, particularly concerning its reliability as no interconnections between the modules are required, avoiding single-point of failure mechanisms, analogous as the P/f and P/V droops. With the frequency-encoding approach, the designer can select the frequency range over which the current-sharing information is communicated and can use this design freedom to achieve objectives such as noise minimization [79].

In [37], a small ac signal is injected in the system as control signal for P and Q (and the distortion current). The control scheme is shown in Fig. 20. For example for Q, the measured Q is drooped with droop $K_{\text{ripple,K}}$ to obtain the frequency f_Q of the ripple component in

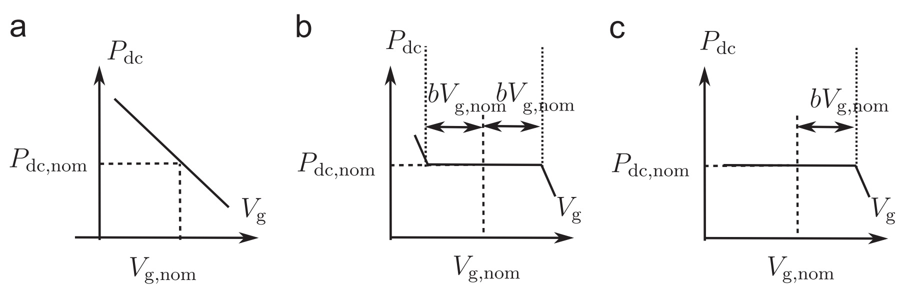

Fig. 18. VBD control: constant-power bands. (a) dispatchable unit, (b) less controllable unit (without storage nor controllable load), and (c) renewable energy source.

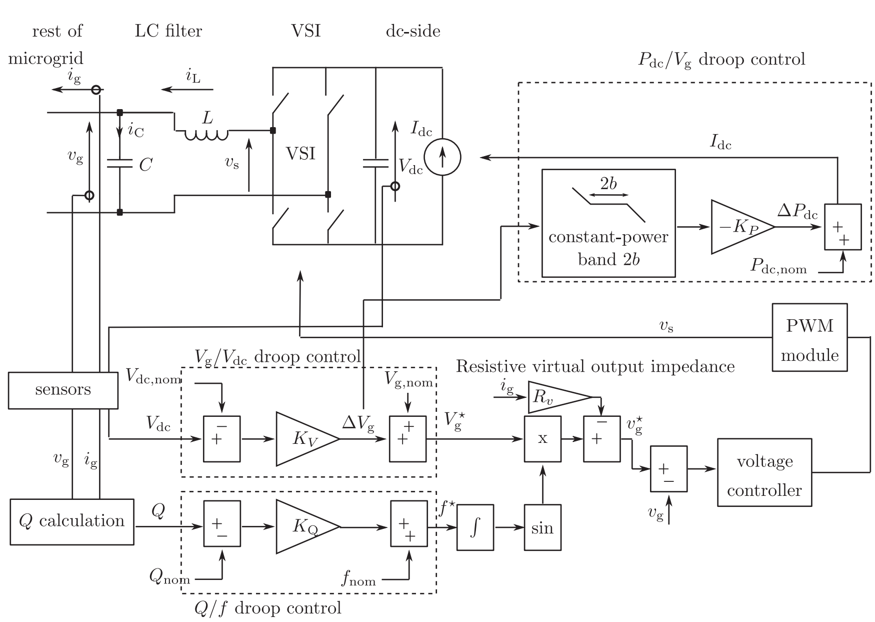

Fig. 19. VBD control: P/V droops and Q/f droops, V_g/V_{dc} droop controller and constant-power bands.

the output voltage:

$$f_Q = f_{Q,0} + K_{\text{ripple,K}} Q \tag{32}$$

A signal $V_q \cos(2\pi f_Q t)$ is added to the reference voltage of for example, 230 V/50 Hz, with V_q a constant value. For two DG units, $f_{Q,1} \approx f_{Q,2}$ such that in the system analysis, phase angle deviations instead of frequency differences can be considered. Hence, if Q_1 increases, then $f_{Q,1} > f_{Q,2}$ and the phase angle of the first unit will keep increasing relatively to that of the second one. From the power flow equations in inductive lines, it follows that the active power at the considered frequency f_Q of the first unit will increase $P_{f_{Q,1}} > P_{f_{Q,2}}$. A PLL is used to measure this frequency component in the current, the voltage is known as it is a controlled variable. With both values, the active power in this frequency component (P_{f_Q}) is obtained. For the reactive power sharing, this active power is drooped to obtain the reference amplitude of the fundamental voltage such that $V_{g,1}$ will decrease:

$$V_{g,1} = V_{g,\text{ref}} - K_Q P_{f_Q} \tag{33}$$

In this way, a Q/V droop is achieved, but indirectly through the frequency component f_Q. A disadvantage of this method is its complexity and the need to measure and generate high-frequency components.

In [37], the harmonic distortion D caused by non-linear loads is shared in an analogous manner. A control signal with a frequency that is drooped with D is injected. The power in this injected control signal is then used to adjust the bandwidth of the voltage loop of the inverter.

In Fig. 21, the method of [79] is depicted. Each module injects into the current-sharing bus a signal with a frequency that is related to its output current/power. The needed perturbations in the output current are generated in the converters under current-mode control. The resulting signal is available for each module. Each module employs a frequency estimator to calculate a weighted average ω_{est} of the frequency content of the aggregate signal [79].

In Fig. 22, the method of [79,80] is depicted where the switching ripple of the modules is used as the perturbation source. Each converter is controlled such that its average current/power is directly related to its switching frequency. The aggregate output ripple voltage contains information about the output of the individual modules. This approach has the benefit that no additional ripple is injected into the output to encode the

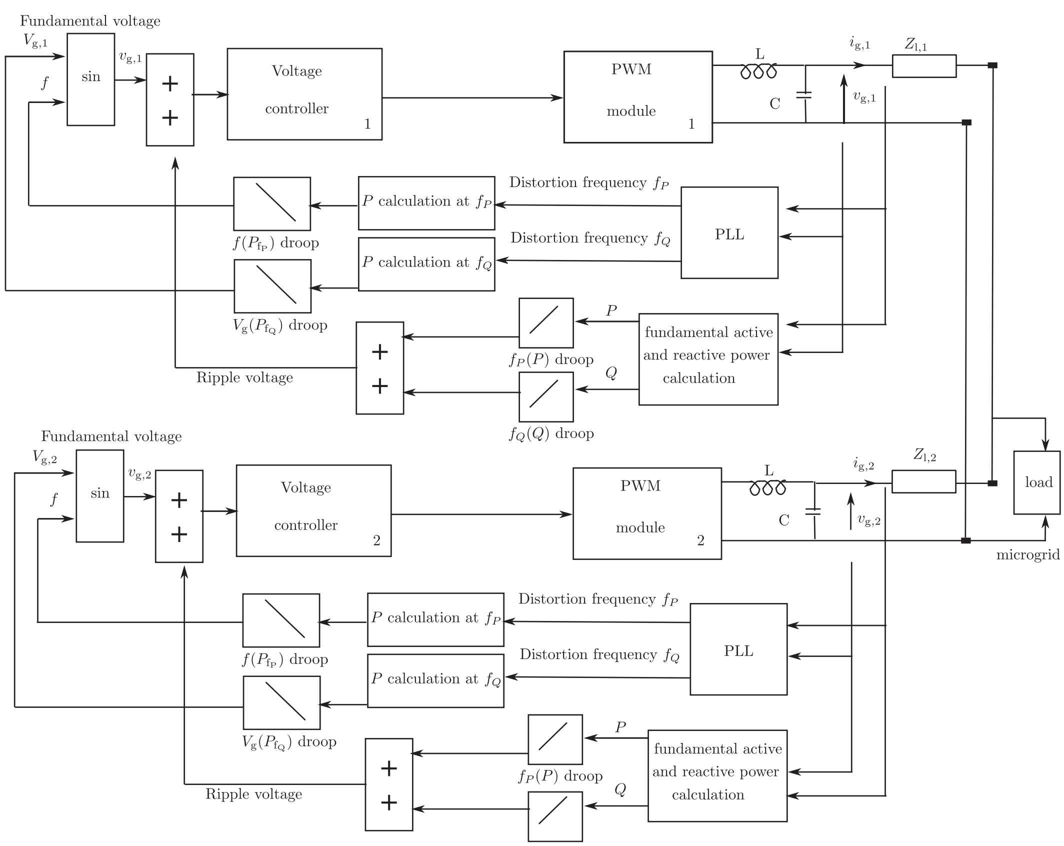

Fig. 20. Frequency based signal injection.

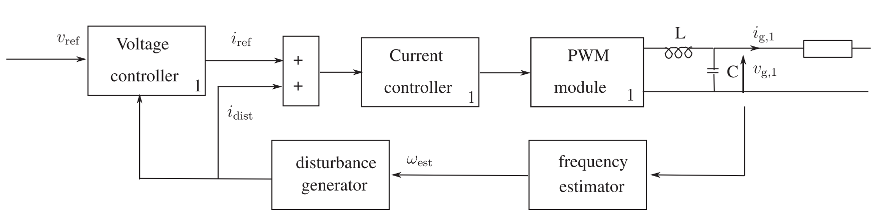

Fig. 21. Frequency based signal injection with perturbation generator.

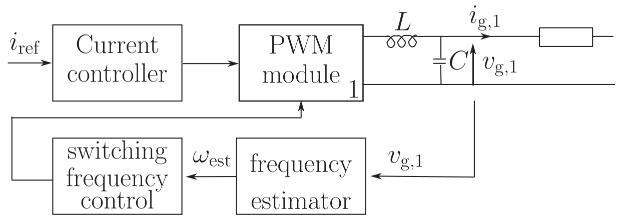

Fig. 22. Frequency based signal injection with changing the switching frequency.

current sharing information, and controlling the switching frequency of the converters is typically straightforward.

6. Hybrid control

Although droop control does not ensure a constant V and f, nor an exact power sharing, its advantage of avoiding control-interconnections makes it a competitive solution [57]. The average current sharing control strategy does need communication, but ensures an accurate V and f control. Therefore, in [57] a hybrid solution combining these two controllers is presented.

7. Conclusions

This paper presents an overview of different primary control strategies for grid-forming converters in islanded microgrids. Detailed control schemes have been included. Central control is a simple and stable strategy providing a good current sharing, but a low reliability and redundancy. Master/slave control achieves good current sharing and stability as well, but depends on the reliability of the master. Droop controllers have been presented to avoid critical communication links, thus, to increase the system's reliability, modularity and flexibility. Some improvements have been done to overcome the inherent drawbacks.

Acknowledgments

The work of T. Vandoorn is financially supported by a Fellowship from the FWO-Vlaanderen (Research Foundation—Flanders, Belgium). The research was carried out in the frame of the Inter-university Attraction Poles programme IAP-VII-43, funded by the Belgian Government. The research of J. D. M. De Kooning is funded by the Special Research Fund (BOF) of Ghent University (Belgium).

References

[1] Engler A, Osika O, Barnes M, Jenkins N, Arulampalam A. DB1 local micro source controller strategies and algorithms. ⟨www.microgrids.eu/micro2000⟩, European Commission, 2004.
[2] Li YW, Kao CN. An accurate power control strategy for power electronics interfaced distributed generation units operating in a low voltage multibus microgrid. IEEE Transactions on Power Electronics 2009;24:2977–88.
[3] Peças Lopes JA, Moreira CL, Madureira AG, Defining control strategies for analysing microgrids islanded operation. In: IEEE St Petersburg Power Tech, Russia.
[4] Blaabjerg F, Teodorescu R, Liserre M, Timbus AV. Overview of control and grid synchronization for distributed power generation systems. IEEE Transactions on Industrial Electronics 2006;53:1398–408.
[5] Ueda F, Matsui K, Asao M, Tsuboi K. Parallel-connections of pulsewidth modulated inverters using current sharing reactors. IEEE Transactions on Power Electronics 1995;10:673–9.
[6] Irving BT, Jovanovic MJ. Analysis, design, and performance evaluation of droop current-sharing method. In: IEEE applied power electronics conference and exposition (APEC), vol. 1, New Orleans, USA, p. 235–41 .
[7] Engler A, Soultanis N. Droop control in LV-grids . In: Proceedings of the international conference on future power systems. The Netherlands.
[8] Engler A. Control of parallel operating battery inverters. In: 1st PV hybrid power systems conference, Aix-en-Provence, France.
[9] Chen J-F, Chu C-L. Combination voltage-controlled and current-controlled PWM inverters for UPS parallel operation. IEEE Transactions on Industrial Electronics 1995;10:547–58.
[10] Siri K, Lee CQ, Wu TF. Current distribution control for parallel connected converters part ii. IEEE Transactions on Aerospace and Electronic Systems 1992;28:841–51.
[11] Wu TF, Siri K, Banda J, The central-limit control and impact of cable resistance in current distribution for parallel-connected DC-DC converters. In: 25th annual IEEE power electronics specialists conference (PESC '94), Taipei, Taiwan, p. 694–702 .
[12] Banda J, Siri K. Improved central-limit control for parallel-operation of dc–dc power converters. In: IEEE power electronics specialists conference (PESC 95), Atlanta, USA, p. 1104–10 .
[13] Prodanović M. Power quality and control aspects of parallel connected inverters in distributed generation. PhD thesis. University of London, Imperial College; 2004.
[14] Kawabata T, Higashino S. Parallel operation of voltage source inverters. IEEE Industry Applications Magazine 1988;24:281–7.
[15] Siri K, Lee CQ, Wu TF. Current distribution control for parallel connected converters part i. IEEE Transactions on Aerospace and Electronic Systems 1992;28:829–40.
[16] Guerrero JM, Hang L, Uceda J. Control of distributed uninterruptible power supply systems. IEEE Transactions on Industrial Electronics 2008;55: 2845–59.
[17] Ramos R, Biel D, Guinjoan F, Fossas E. Master–slave sliding-mode control design in parallel-connected inverters. Automatica 2001;42:37–44.
[18] Petruzziello F, Ziogas PD, Joos G. A novel approach to paralleling of power converter units with true redundancy. In: The 21st annual IEEE power and electron specialists conference, San Antonio, TX, USA.
[19] Holtz J, Werner K. Multi-inverter UPS system with redundant load sharing control. IEEE Transactions on Industrial Electronics 1990;37:506–13.
[20] Lee W-C, Lee T-K, Lee S-H, Kim K-H, Hyun D-S, Suh I-Y . A master and slave control strategy for parallel operation of three-phase UPS systems with different ratings. In: Proceedings of the IEEE the applied power electronics conference and exposition (APEC'04), California, p. 456–62 .
[21] Uninterruptible power supplies and active filters. CRC Press; 2005.
[22] Lee WC, Lee SH, Kim KH, Hyun DS. Novel control strategy for parallel operation of UPS system. In: 4th internat power electronics and motion control conference (IPEMC'04), vol. 2, Xi'an, China, p. 983–8 .
[23] Pei Y, Jiang G, Yang X, Wang Z. Auto-master–slave control technique of parallel inverters in distributed AC power systems and UPS. In: 35th annual IEEE power electronics specialists conference, Aachen, Germany.
[24] Sun X, Lee Y-S, Xu D. Modeling, analysis, and implementation of parallel multi-inverter systems with instantaneous average-current-sharing scheme. IEEE Transactions on Power Electronics 2003;18:844–56.
[25] Xing Y, Huang L, Yan Y. Redundant parallel control for current regulated inverters with instantaneous current sharing. In: IEEE 34th annual power electronics specialist conference (PESC'03), vol. 3, Acapulco, Mexico, p. 1438–42 .
[26] Roslan AM, Ahmed KH, Finney SJ, Williams BW. Improved instantaneous average current-sharing control scheme for parallel-connected inverter considering line impedance impact in microgrid networks. IEEE Transactions on Power Electronics 2011;26:702–16.
[27] Chen Y-K, Wu Y-E, Wu T-F, Ku C-P. ACSS for paralleled multi-inverter systems with DSP-based robust controls. IEEE Transactions on Aerospace and Electronic Systems 2003;39:1002–15.
[28] Shan H, Kang Y, Duan S, Zhang Y, Yu M, Liu Y, et al. Research on a novel digital parallel current sharing control technique of modularized ups. In: International conference on electrical machines and systems, Seoul, Korea, p. 106–9 .
[29] Fang T, Ruan X, Xiao L, Liu A. An improved distributed control strategy for parallel inverters. In: Power electronics specialist conference (PESC'08), Island of Rhodes, Greece, p. 3500–5 .
[30] Chen Y-K, Wu Y-E, Wu T-F, Ku C-P . CWDC strategy for paralleled multi-inverter systems achieving a weighted output current distribution. In: 17th annual IEEE applied power EL conference and exposition (APEC), Dellas, Texas, p. 1018–23 .
[31] Chen Q, Ju P, Shi KQ, Tang Y, Shao ZY, Yang WY. Parameter estimation and comparison of the load models with considering distribution network directly or indirectly. Electric Power Systems Research 2010;32.
[32] Chen C-L, Wang Y, Lai J-S, Lee Y-S, Martin D. Design of parallel inverters for smooth mode transfer microgrid applications. IEEE Transactions on Power Electronics 2010;25:6–15.
[33] Wu T-F, Chen Y-K, Huang Y-H. 3C strategy for inverters in parallel operation achieving an equal current distribution. IEEE Transactions on Industrial Electronics 2000;47:273–81.
[34] Prodanović M, Green TC. High-quality power generation through distributed control of a power park microgrid. IEEE Transactions on Industrial Electronics 2006;53:1471–82.
[35] Majumder R, Chaudhuri B, Ghosh A, Majumder R, Ledwich G, Zare F. Improvement of stability and load sharing in an autonomous microgrid using supplementary droop control loop. IEEE Transactions Power Systems 2010;25:796–808.
[36] Barsali S, Ceraolo M, Pelacchi P, Poli D. Control techniques of dispersed generators to improve the continuity of electricity supply. In: Proceedings of the IEEE PES winter meeting, p. 789–94 .

[37] Tuladhar A, Jin H, Unger T, Mauch K. Control of parallel inverters in distributed AC power systems with consideration of line impedance effect. IEEE Transactions on Industry Applications 2000;36:131–8.
[38] Barklund E, Pogaku N, Prodanović M, Hernandez-Aramburo C, Green TC. Energy management in autonomous microgrid using stability-constrained droop control of inverters. IEEE Transactions on Power Electronics 2008;23: 2346–52.
[39] Lasseter RH, Paigi P. Microgrid: a conceptual solution. In: Proceedings of the IEEE power electron special conference (PESC 2004), Aachen, Germany.
[40] Engler A, Osika O, Barnes M, Hatziargyriou N. DB2 Evaluation of the local controller strategies, 〈www.microgrids.eu/micro2000〉, 2005.
[41] Marwali M, Jung J-W, Keyhani A. Control of distributed generation systems—part II: load sharing control. IEEE Transactions on Power Electronics 2004;19: 1551–61.
[42] Katiraei F, Iravani R, Hatziargyriou N, Dimeas A. Microgrids management: controls and operation aspects of microgrids. Power and Energy Magazine 2008;6:54–65.
[43] Chandorkar MC, Divan DM, Adapa R. Control of parallel connected inverters in standalone AC supply systems. IEEE Transactions Industry Applications 1993;29:136–43.
[44] Bhuiyan FA, Yazdani A. Multimode control of a DFIG-Based wind-power unit for remote applications. IEEE Transactions on Power Delivery 2009;24: 2079–89.
[45] Arboleya P, Diaz D, Guerrero JM, Garcia P, Briz F, Gonzalez-Moran C, et al. An improved control scheme based in droop characteristic for microgrid converters. Electric Power Systems Research 2010;80:1215–21.
[46] Guerrero JM, Matas J, García de Vicuña L, Castilla M, Miret J. Wireless-control strategy for parallel operation of distributed-generation inverters. IEEE Transactions on Industrial Electronics 2006;53:1461–70.
[47] Guerrero JM, Vásquez JC, Matas J, García de Vicuña L, Castilla M. Hierarchical control of droop-controlled AC and DC microgrids—a general approach towards standardization. IEEE Transactions on Industrial Electronics 2011;58: 158–72.
[48] Guerrero JM, García de Vicuña L, Matas J, Castilla M, Miret J. Output impedance design of parallel-connected UPS inverters with wireless load-sharing control. IEEE Transactions on Industrial Electronics 2005;52: 1126–35.
[49] Katiraei F, Iravani MR. Power management strategies for a microgrid with multiple distributed generation units. IEEE Transactions on Power Systems 2006;21:1821–31.
[50] Guerrero JM, Matas J, García de Vicuña L, Castilla M, Miret J. Decentralized control for parallel operation of distributed generation inverters using resistive output impedance. IEEE Transactions on Industrial Electronics 2007;54: 994–1004.
[51] Mohamed Y, El-Saadany EF. Adaptive decentralized droop controller to preserve power sharing stability for paralleled inverters in distributed generation microgrids. IEEE Transactions on Power Electronics 2008;23: 2806–16.
[52] Guerrero JM, Vásquez JC, Matas J, Castilla M, García de Vicuña L. Control strategy for flexible microgrid based on parallel line-interactive UPS systems. IEEE Transactions on Industrial Electronics 2009;56:726–36.
[53] Vasquez JC, Mastromauro RA, Guerrero JM, Liserre M. Voltage-support provided by a droop-controlled multifunctional inverter. IEEE Transactions on Industrial Electronics 2009;56:4510–9.
[54] Matas J, Castilla M, de Vicuña LG, Vasquez JC. Virtual impedance loop for droop-controlled single-phase parallel inverters using a second order general integrator scheme. IEEE Transactions on Power Electronics 2010;25:2993.
[55] Debrabandere K, Bolsens B, Van den Keybus J, Woyte A, Driesen J, Belmans R. A voltage and frequency droop control method for parallel inverters. IEEE Transactions on Power Electronics 2007;22:1107–15.
[56] Lee C-T, Chuang C-C, Chu C-C, Chang P-T . Control strategies for distributed energy resources interface converters in the low voltage microgrid. In: IEEE energy conversion congress and exposition (ECCE 2009), San Jose, CA.
[57] Yu X, Wang HH, Khambadkone AM, Sing ST. A hybrid control architecture for low voltage microgrid. In: IEEE energy conversion congress and exposition (ECCE 2010), Atlanta, GA, p. 3161–8 .
[58] Li Y, Li YW. Decoupled power control for an inverter based low voltage microgrid in autonomous operation. In: IEEE 6th internat electron and motion control conference (IPEMC'09), Wuhan, China, p. 2490–6 .
[59] Li Y, Li YW. Power management of inverter interfaced autonomous microgrid based on virtual frequency–voltage frame. IEEE Transactions on Smart Grid 2011;2:30–40.
[60] Vasquez JC, Guerrero JM, Luna A, Rodriguez P, Teodorescu R. Adaptive droop control applied to voltage-source inverters operating in grid-connected and islanded modes. IEEE Transactions on Industrial Electronics 2009;56: 4088–96.
[61] Lee T-L, Cheng P-T. Design of a new cooperative harmonic filtering strategy for distributed generation interface converters in an islanding network. IEEE Transactions on Power Electronics 2007;2:1919–27.
[62] Akagi H, Kanagawa Y, Nabase A. Instantaneous reactive power compensator comprising switching devices without energy storage components. IEEE Transactions on Industrial Applications 1984;20:625–30.
[63] Tuladhar A, Jin H, Unger T, Mauch K. Parallel operation of single phase inverter modules with no control interconnections. In: Applied power electronics conference and exposition 1997 (APEC'97), Atlanta, GA, USA.
[64] Vrana TK, Hille C. A novel control method for dispersed converters providing dynamic frequency response. Electrical Engineering Journal, Springer-Verlag 2011;93:217–26.
[65] Driesen J, Visscher K. Virtual synchronous generators. In: Proceedings of the IEEE PES general meeting, Pittsburgh, PA, USA.
[66] Visscher K. Vsync—the virtual synchronous generator concept; 2008.
[67] Sakimoto K, Miura Y, Ise T. Stabilization of a power system with a distributed generation by a virtual synchronous generation function. In: 8th international conference on power electronics (ECCE), Korea.
[68] Beck H-P, Hesse R. Virtual synchronous machine. In: 9th international conference on electrical power quality and utilisation (EPQU2007), Barcelona, Spain.
[69] Hesse R, Turschner D, Beck H-P . Micro grid stabilisation using the Virtual Synchronous Machine (VISMA). In: International conference on renewable energies and power quality (ICREPQ'09), Valencia, Spain.
[70] Zhong Q-C, Weiss G. Synchronverters: inverters that mimic synchronous generators. IEEE Transactions on Industrial Electronics 2011;58:1259–67.
[71] Yan D, Jianhui S, Yong S. A unified power controller for photovoltaic generators in microgrid. In: 4th international conference on electric utility deregulation and restructuring and power technologies (DRPT2011), Weihai, China, p. 1121–5 .
[72] Du Y, Su J, Mao M, Yang X. Autonomous controller based on synchronous generator dq0 model for micro grid inverters. In: 8th international conference on power electronics (ECCE Asia), The Shilla Jeju, Korea.
[73] Sao C, Lehn P. Intentional islanded operation of converter fed microgrids. In: Proc IEEE power engineering society general meeting; 2006.
[74] Sao C, Lehn P. Control and power management of converter fed microgrids. IEEE Transactions on Power Systems 2008;23.
[75] Au-Yeung J, Vanalme GMA, Myrzik JMA, Karaliolios P, Bongaerts M, Bozelie J et al. Development of a voltage and frequency control strategy for an autonomous LV network with distributed generators. In: The 44th international universities' power engineering conference (UPEC 2009), Glasgow, Scotland.
[76] Savaghebi M, Jalilian A. A new control strategy for distributed generation interface converters to compensate for microgrid harmonics. In: International symposium on power electronics, electrical drives, automation and motion (SPEEDAM2010), Pisa, Italy, p. 908–13 .
[77] Vandoorn TL, Meersman B, Degroote L, Renders B, Vandevelde L. A control strategy for islanded microgrids with DC-link voltage control. IEEE Transactions on Power Delivery 2011;26:703–13.
[78] Vandoorn TL, Meersman B, Kooning JDMD, Vandevelde L. Controllable harmonic current sharing in islanded microgrids: Dg units with programmable resistive behavior towards harmonics. IEEE Transactions Power Delivery 2012;27: 831–41.
[79] Perreault DJ, Selders RL, Kassakian JG. Frequency-based current-sharing techniques for paralleled power converters. IEEE Transactions on Power Electronics 1998;13:626–34.
[80] Perreault DJ, Sato K, Selders RL, Kassakian JG. Switching-ripple-based current sharing for paralleled power converters. IEEE Transactions on Circuits and Systems I 1999;46:1264–74.